Frontiers of Information Technology & Electronic Engineering
www.jzus.zju.edu.cn; engineering.cae.cn; www.springerlink.com
ISSN 2095-9184 (print); ISSN 2095-9230 (online)
E-mail: jzus@zju.edu.cn

# Ultra-low-power backscatter-based software-defined radio for intelligent and simplified IoT network*

Huixin DONG[1], Wei KUANG[1], Fei XIAO‡[2], Lihai LIU[3],
Feng XIANG[4], Wei WANG[1], Jianhua HE[5]

[1]*School of Electronic Information and Communication, Huazhong University of Science and Technology, Wuhan 430074, China*

[2]*School of Management, Huazhong University of Science and Technology, Wuhan 430074, China*

[3]*China Railway Siyuan Survey and Design Group Co., Ltd., Wuhan 430063, China*

[4]*Wuhan Maritime Communication Research Institute, Wuhan 430079, China*

[5]*School of Computer Science and Electronic Engineering, University of Essex, Colchester CO4 3SQ, UK*

E-mail: huixin@hust.edu.cn; kuangwei@hust.edu.cn; feixiao@hust.edu.cn; isaacllh@hotmail.com; fengxiang@alumni.hust.edu.cn; weiwangw@hust.edu.cn; j.he@essex.ac.uk

Received July 2, 2021; Revision accepted Nov. 11, 2021; Crosschecked Dec. 1, 2021

**Abstract:** The recent decade has witnessed an upsurge in the demands of intelligent and simplified Internet of Things (IoT) networks that provide ultra-low-power communication for numerous miniaturized devices. Although the research community has paid great attention to wireless protocol designs for these networks, researchers are handicapped by the lack of an energy-efficient software-defined radio (SDR) platform for fast implementation and experimental evaluation. Current SDRs perform well in battery-equipped systems, but fail to support miniaturized IoT devices with stringent hardware and power constraints. This paper takes the first step toward designing an ultra-low-power SDR that satisfies the ultra-low-power or even battery-free requirements of intelligent and simplified IoT networks. To achieve this goal, the core technique is the effective integration of μW-level backscatter in our SDR to sidestep power-hungry active radio frequency chains. We carefully develop a novel circuit design for efficient energy harvesting and power control, and devise a competent solution for eliminating the harmonic and mirror frequencies caused by backscatter hardware. We evaluate the proposed SDR using different modulation schemes, and it achieves a high data rate of 100 kb/s with power consumption less than 200 μW in the active mode and as low as 10 μW in the sleep mode. We also conduct a case study of railway inspection using our platform, achieving 1 kb/s battery-free data delivery to the monitoring unmanned aerial vehicle at a distance of 50 m in a real-world environment, and provide two case studies on smart factories and logistic distribution to explore the application of our platform.

**Key words:** Backscatter; Ultra-low-power SDR; IoT networks
https://doi.org/10.1631/FITEE.2100321 **CLC number:** TN926

## 1 Introduction

Due to the high energy efficiency and low maintenance cost, intelligent and simplified Internet of Things (IoT) networks have recently gained a lot of attention in emerging applications, such as smart factories and logistics (Zhao RJ et al., 2020). Unlike traditional communication networks, intelligent and

‡ Corresponding author
* Project supported by the National Key R&D Program of China (Nos. 2020YFB1806606 and 2016YFB1200100) and the National Natural Science Foundation of China (No. 62071194)
ORCID: Huixin DONG, https://orcid.org/0000-0002-5984-9194; Fei XIAO, https://orcid.org/0000-0003-0889-1779

simplified IoT networks, a part of the future "intellicise" wireless network (Zhang P et al., 2022), require a stricter power constraint and the orchestration of existing commodity devices, which cannot be satisfied by traditional software-defined radio (SDR) platforms such as Universal Software Radio Peripherals (USRPs) (Ettus, 2018). To deal with this problem, researchers have to develop dedicated hardware platforms or use software simulation for algorithm implementations, which hinders their fast implementation and experimental evaluation. To embrace the coming wave of intelligent and simplified IoT networks, it is important to develop a novel SDR platform that can support ultra-low-power communication.

Although many efforts have been devoted to developing low-power SDRs, existing solutions still rely on a stable power supply. μSDR (Kuo et al., 2012) adopts power-efficient narrow-band radio frequency (RF) chips to save energy. TinySDR (Hessar et al., 2020) reduces communication overhead by dynamically switching between active and sleep modes. However, to facilitate ultra-low-power communications, miniaturized IoT devices are basically powered by opportunistic energy-harvesting schemes and thus have an unstable power supply, which cannot be supported by traditional power-stable SDRs.

Driven by the need for an energy-efficient SDR platform, we propose a lightweight SDR platform for simplified and intelligent IoT networks, as shown in Fig. 1. This platform provides a low-power solution for a backscatter-driven RF front end with μW-level power consumption. Furthermore, it works on the 900 MHz industrial, scientific, and medical (ISM) band and has multiple interfaces for sensor connection.

Realizing such an SDR involves the following challenges:

1. Low-power hardware architecture. A key challenge in realizing our design is how to competently reduce the system's overall power consumption. On one hand, we integrate a competitive energy-harvesting circuit into our system for more power supply. On the other hand, to achieve less power consumption, we turn to a backscatter-driven RF front end instead of directly using a conventional multiplier and power amplifier. In particular, we build an SDR that modulates signals from ambient environments for data delivery. We will address this challenge in Section 3.1, and the power consumption is achieved as low as 10 μW in the sleep mode.

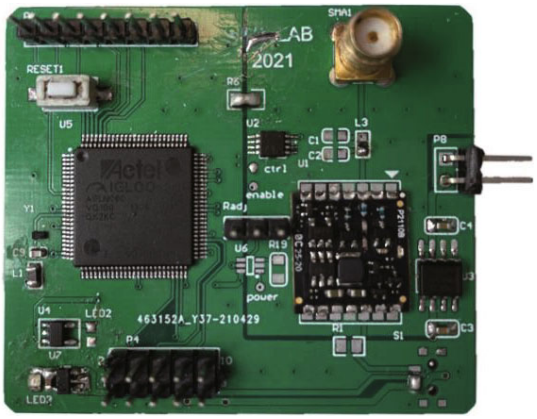


**Fig. 1 Battery-free backscatter platform for IoT networks**

2. Harmonic and mirror frequencies. The other challenge is how to eliminate unwanted interference from backscattering operations. Specifically, backscatter communications work by intermittently switching between different impedance states, which results in noisy harmonic and mirror frequency components in the received signal. To deal with this problem, we use multi-level impedance to improve the precision of waveform synthesis. For each selected impedance, the absolute values of its real and imaginary parts should be equal, to eliminate harmonic and mirror frequencies.

We evaluate the proposed SDR using different modulation schemes with a bit rate up to 500 kb/s. Specifically, our platform achieves almost the same bit error rate (BER) as traditional SDRs with the same signal-to-noise ratio (SNR) under ASK modulation. Furthermore, our platform can be fully charged in 60 s at a distance of 1 m. We also present a case study of our platform for railway inspection. In this study, our system achieves 1 kb/s battery-free data delivery to the monitoring unmanned aerial vehicle (UAV) at a distance of 50 m in real-world tests.

The contributions of this paper are as follows:

1. We provide a thoughtful study toward enabling power-efficient SDRs that satisfy the ultra-low-power or even battery-free requirements of intelligent and simplified IoT networks.

2. We explore the fundamental structure of the backscatter-based SDR platform, carefully develop a novel circuit design for efficient energy harvesting and power control, and successfully cancel the harmonic and mirror frequencies.

3. We implement our system and quantify the performance of our design in a real-world scenario.

## 2 Power-efficient wireless communication systems for IoT nodes

In this section, we explore power-efficient wireless communication systems for IoT nodes. First of all, we hope to convince readers that energy efficiency is absolutely essential for IoT. For IoT terminal nodes that need to be deployed in an outdoor environment, regular charging and battery replacement costs are relatively high. Expensive components thwart wide promotion of IoT networks. Although existing platforms have not focused on energy harvesting or management, their hardware structure inspires our system design. Here, we analyze the current platforms related to power-efficient IoT nodes.

### 2.1 Low-power SDR platforms

Many commercial and open-source SDR platforms assist developers in testing the communication protocols and performance before mass production. There are many low-power SDR commercial platforms that researchers widely use. Cable-powered SDR platforms including μSDR (Kuo et al., 2012), USRP B200mini (Ettus, 2018), and LimeSDR mini (LimeNet, 2018) usually need to connect to a personal computer for power supply and data processing.

Standalone SDRs powered by batteries like TinySDR (Hessar et al., 2020) are designed for IoT terminal nodes. They reduce costs and power consumption using the same narrow bandwidth as the IoT terminal nodes for communication, but do not consider scenarios with unstable power supply.

Existing SDRs are stable only when they are powered by cables or batteries, which indicates that they are unfit for implementation with strict sleep and active modes. Although we have observed that energy harvesting and management are essential for ultra-low-power IoT nodes, under actual working conditions, the power supply from the environment is unstable. Our goal is to design a low-power, inexpensive SDR that can work independently. We compare the power consumption and cost parameters of several common SDRs in Table 1. The result indicates the superiority of our design in power efficiency over existing SDR platforms.

**Table 1 Comparision between different SDR platforms**

| Platform | Sleep power | Standalone | Cost |
|---|---|---|---|
| USRP B200mini | Not support | No | $733 |
| LimeSDR mini | Not support | No | $159 |
| PlutoSDR | Not support | No | $159 |
| μSDR | 320 mW | Yes | $149 |
| Galiot | 350 mW | Yes | $60 |
| TinySDR | 33 μW | Yes | $55 |
| Our design | 10 μW | Yes | $60 |

### 2.2 Multi-protocol backscatter platforms

As an emerging communication technology, backscatter takes advantages of low power consumption and low cost, and is suitable for the deployment of large-scale IoT nodes. Nowadays, there are many research groups that attempt to develop backscatter communication platforms. For example, the open-source project WISP (Philipose et al., 2005) is a passive programmable ultra-high frequency radio frequency identification (RFID) communication platform that is compatible with the EPC Gen2 protocol of RFID. HitchHike (Zhang PY et al., 2016) provides a solution for backscatter to communicate with WiFi, and LoRa backscatter (Talla et al., 2017) and PLoRa (Peng et al., 2018) provide solutions for connecting to commercial LoRa gateways.

These works provide us with many technical references, but they do not target energy-efficient IoT networks. We are the first to use backscatter as an SDR platform with an energy harvesting and management system.

## 3 System design

In this section, we describe the hardware components of our system and introduce the power management scheme that achieves ultra-low power consumption. Then, we describe the control method for realizing the primary modulation such as amplitude modulation (AM), phase modulation (PM), and frequency modulation (FM). Finally, we present our approach for realizing network management.

First, we would like to address the question of whether wireless signal modulation can be achieved when high-power devices such as local oscillators, multipliers, and RF power amplifiers are eliminated. We will briefly explain why an RF switch can be used to achieve modulation of the wireless signal.

After the electromagnetic wave signal is received by the antenna, it enters the internal circuit. If the impedance of the internal circuit matches the impedance of the antenna, and the maximum power transmission theorem is satisfied, the signal energy is coupled into the internal circuit to the greatest extent, and it is in the absorption state at this time. When the internal circuit impedance does not match the antenna impedance, a part of the signal is reflected. This part of the reflected signal can be described by the following reflection coefficient equation:

$$\Gamma = \frac{Z_{\mathrm{S}} - Z_{\mathrm{L}}}{Z_{\mathrm{S}} + Z_{\mathrm{L}}}, \tag{1}$$

where $Z_{\mathrm{S}}$ is the antenna impedance and $Z_{\mathrm{L}}$ is the impedance of the matching circuit. By controlling the impedance, we can control the amplitude and phase of the reflected electromagnetic wave, which will modulate the signal on the carrier.

However, the use of reflected electromagnetic waves to achieve signal modulation has difficulties. Compared with the modulation method, where the multiplier can achieve direct signal synthesis, the quantization accuracy of the backscatters technology is far from sufficient. This is also our first challenge in using backscattering devices to achieve modulation. That is, traditional backscatters can generate a signal at the desired frequency, but will cause harmonic and mirror copies as well.

To solve this problem, we design eight kinds of impedances and corresponding control logic. The real and imaginary parts of these eight impedances' reflection coefficients are orthogonal to each other, which approximates complex signal $e^{jx}$, and backscatter communication realized in this way can suppress the undesired signal.

The other challenge is to achieve normal wake-up and work when the power supply is unstable. For example, when an energy-harvesting system is used to power the system, it is limited by changes in the electromagnetic energy density in the environment. Ensuring that the system can wake up and communicate is necessary.

We design our platform with the lowest-power-consumption components, such as the low-power controller AGLN250, low-power oscillator SiT1576 for field-programmable gate arrays (FPGAs), and energy-harvesting module P2110B with a matching network. We also design low-power operating modes and energy management systems to improve the energy efficiency.

### 3.1 Hardware design

The hardware system design of our platform is presented in Fig. 2. Under the premise of ensuring normal function, our hardware design should reduce the system's power consumption as much as possible, so it is essential to select proper components.

#### 3.1.1 FPGA

As the controller of the entire system, the FPGA should have enough computing resources to ensure normal operation of the designed program scheme

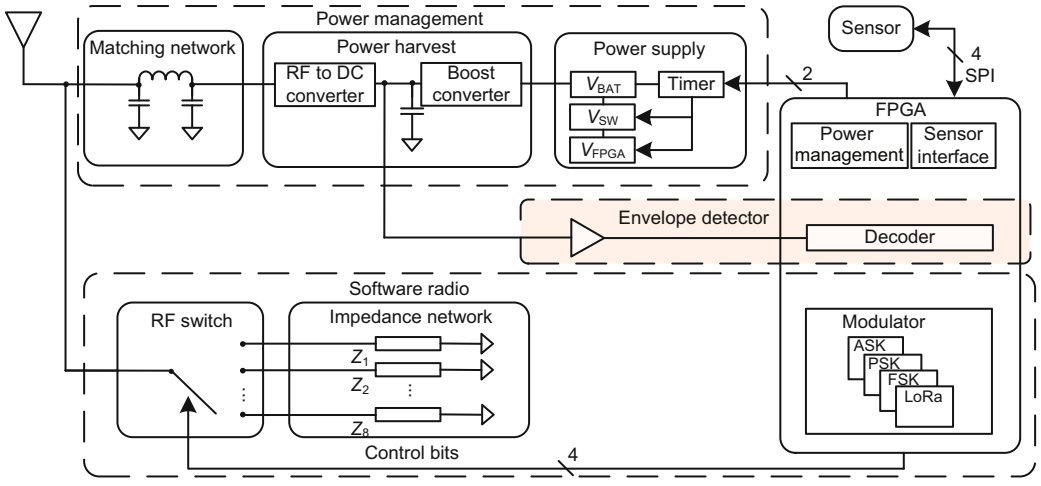


**Fig. 2 Hardware system block diagram**

and have low enough energy consumption to meet the energy constraint to complete the task of sending a large data packet. Considering that the platform is working in the duty-cycle mode, the FPGA should support fast wake-up as well. Therefore, we choose the IGLOO Nano AGLN250 FPGA from Microsemi for baseband processing, which is flash-based and has 6144 versal tiles. The chip also has the lowest power consumption in the industry and can be as low as 2 μW in the sleep mode (Microsemi, 2012).

#### 3.1.2 RF switch

The RF switch needs to satisfy aspects such as operating frequency band, insertion loss, and cost. Our solution for modulation should toggle eight boundary impedances of the antenna by RF switch, so SP8T or cascaded SP4T switches that can control eight channels are needed. Some commonly used RF switches are found on ADI's website, such as the SP8T chips (such as HMC253 and HMC322) and SP4T chips (such as ADG904). The operating frequency band of these switches corresponds to the frequency band of IoT devices, and the insertion loss of these switches is acceptable. However, all SP8Ts have high power consumption and require a 5-V power supply, which is contrary to our desire for low power. The ADG904, with a maximum working electric current of 1 μA (Analog Devices, 2016), becomes our first choice. We choose cascaded ADG904 SP4T switches to create an SP8T switch network instead.

#### 3.1.3 Oscillator

The FPGA operation requires an external oscillator to provide a stable clock source, but this also means that the crystal oscillator will work throughout the working cycle. Therefore, we choose SiT1576 based on the low-power microelectromechanical system (MEMS) technology. The crystal oscillator current is only 6 μA at an output of 100 kHz (SiTime, 2017).

#### 3.1.4 Timer

Timer is the key part of achieving a low-power duty-cycle working mode. It needs to be active continually, so we choose the ultra-low-power timer chip TPL5111 produced by TI, whose power consumption is only 65 nW (TI, 2018a).

In summary, we list the power consumption and cost of each component in Table 2. Among them, the FPGA, oscillator, timer, and RF switch are the most energy-hungry components. We choose to close these components in sleep mode to ensure the overall low power consumption of the system. The P2110B and AVXbest Cap are used for energy harvesting, and provide the energy for the system. The leakage current of the super capacitor is approximately 5 μW (Avx, 2020). The leakage current of the muRata lumped elements is less than 5 nA (muRata, 2018), and two resistances are used for voltage division with 1-μA current in sleep mode. Thus, the overall power consumption of the lumped components is approximately 2 μW. The leakage current of the low dropout regulators (LDOs) is approximately 0.5 μA (TI, 2018b), which indicates 1.5 μW power consumption in sleep mode. Thus, the overall power consumption of our system is approximately 10 μW. In addition, the total cost listed in Table 2 is $60 for the proposed scheme according to the prices of the individual components.

### 3.2 Power management

Now we introduce the power management design of the platform. Because the entire platform is

**Table 2 Bom table of the platform**

| Component | Sleep power | Active power | Cost | Description |
|---|---|---|---|---|
| AGLN250 | Shut down | 200 μW | $10 | FPGA |
| ADG904 | Shut down | 5.4 μW | $6 | RF switch |
| SiT1576 | Shut down | 10.8 μW | $1 | Oscillator |
| TPL5111 | 65 nW | 65 nW | $0.5 | Timer |
| P2110B | | | $35 | Energy harvester |
| AVXbest Cap | 5 μW | | $5.4 | Super-capacitor |
| TPS78218 | 1.5 μW | 1.5 μW | $0.2 | LDO |
| TPS73612 | 1.5 μW | 1.5 μW | $0.8 | LDO |
| Lumped elements | 2 μW | 2 μW | $0.1 | |

battery-free, it is necessary to collect the electromagnetic energy of the excitation source and store it in a super-capacitor to power the system. Due to the limited energy, the platform must work in a duty-cycle mode and reduce the power leakage when the system is in the sleep mode.

#### 3.2.1 Timer mechanism

The duty-cycle working mode is achieved by a timer chip. The timer controls the enable pin of the system's voltage regulator chips. The regulator is enabled according to the cycle time designed by the timer's external circuit, and the system begins to work after power-on. After the data packets are sent, the FPGA controls the timer to disable regulators, and the system falls into sleep mode and collects energy. By equating the energy harvested and working power consumption, the duty cycle of the system is given as

$$\text{Duty} = \frac{T_{\text{on}}}{T_{\text{on}} + T_{\text{sleep}}} = \frac{P_{\text{receive}} \cdot \eta - P_{\text{q}}}{P_{\text{active}}}, \quad (2)$$

where $T_{\text{on}}$ is the duration time, $T_{\text{sleep}}$ is the sleep time, $P_{\text{receive}}$ is the power received by the antenna, $\eta$ is the power harvesting efficiency of the P2110B and can be found in the datasheet, $P_{\text{q}}$ is the quiet power consumption during sleep mode, and $P_{\text{active}}$ is the average power consumption during operation mode. It can be estimated that when receiving $-10$ dBm energy at 915 MHz, the duty can be about $\frac{1}{10}$, which means that if the platform sends a packet that requires 1 s for transmission, it should sleep for at least 9 s to store enough energy.

#### 3.2.2 Energy-harvesting circuit

Our platform uses energy-harvesting module P2110B to collect power from the RF signal from air with the AVXbest super-capacitor for temporary energy storage. When the capacitor reaches the voltage threshold, the module outputs the designed voltage set by the external circuit. The impedance matching network at the radio front end ensures the maximum transmission of the power received by the antenna to the module.

#### 3.2.3 Power domains

The ideal situation is that each device works on its lowest working voltage to obtain the lowest operation power. This means that more regulators will be brought in, causing increased power loss in regulators, higher costs, and more communication mismatches between the controller and peripherals. Therefore, we choose the chips with the working voltage close to the lowest one in our platform.

Power domain $V_1$ is 2.1 V. $V_1$ is the designed output of the energy-harvesting module, which serves as the battery supply of the system and powers the timer chip. The setting of 2.1 V is close to the timer's lowest voltage and reduces the voltage drop in the linear regulator, which can reduce the power dissipation caused by the regulator's low efficiency.

Power domain $V_2$ is 1.8 V. $V_2$ is determined by the FPGA input/output (IO) port supply rule and powers the RF switches and the oscillator. All peripherals use the same voltage to guarantee consistency of the interface and avoid misreading. $V_2$ is generated by the regulator and will be turned off by the timer after data transmission is finished.

Power domain $V_3$ is 1.2 V. The FPGA core supply rule determines $V_3$, and the timer will turn off the power supply after the data transmission is completed.

In addition, we distribute the used pins in the same IO bank and turn off other IO banks' supply to further reduce energy loss.

### 3.3 Modulation scheme

Next, we present our modulation algorithm to achieve primary modulations such as AM, PM, and FM.

#### 3.3.1 Symbol generation

Backscatter technology uses the electromagnetic signal in the environment as a carrier wave and uses the reflection of the antenna to achieve multiplicative modulation. When generating symbols, the FPGA controls the RF switches to change the impedance connected to the antenna, which changes the reflection coefficient of the antenna to designed values at the designed frequency.

To realize amplitude modulation, we divide the impedances into different pairs according to the distance between their reflection coefficients. The controller chooses different pairs to switch, representing different amplitude modulation symbols.

To realize frequency modulation, we should

arrange the eight impedances, whose reflection coefficients are in counterclockwise order, and switch among them, one by one, at a frequency which is eight times the target frequency. Different target frequencies represent different frequency modulation symbols.

To realize phase modulation, we arrange the impedances as frequency modulations. Then we choose different impedances as the beginning point; the beginning point's reflection coefficient has a different phase and will decide the beginning phase of the modulated signal. Changes in the beginning points lead to phase modulation.

Algorithms are listed in Algorithms 1, 2, and 3. Other modulations based on AM, FM, and PM can be realized as well, such as LoRa. We will not discuss them here.

#### 3.3.2 Compatibility setting

Actual deployment is a problem because existing IoT devices may have their own coding rules. Modulating information on the LoRa signal is different with modulating information on WiFi signals. Therefore, the FPGA must have slight changes in source coding and channel coding before the modulation, to meet the communication requirements. Then the FPGA controls the RF switch in the right way and completes the data transmission.

### 3.4 Network management

We now introduce the methods used in network organization and management of our platform in practical deployment.

#### 3.4.1 Downlink and MAC protocol

We adopt a simple MAC protocol to implement the gateway's access control to the platform, and use an envelope detector for downlink communication from the gateway to the IoT node, which is represented by our SDR platform. Each platform in the network holds a unique 8-bit local MAC address. When the gateway needs to specify a platform to send data, it controls the excitation source to turn off the output, which will generate a falling edge in the envelope detector to inform the node to start to deliver the message. Then the gateway sends the MAC address by toggling the excitation source, and the corresponding platform starts to transmit data. In contrast, other platforms turn to the standby mode to store energy and wait for the next connection.

#### 3.4.2 Frame structure

The structure of the data frame sent by the platform is shown in Fig. 3, including the preamble, synchronization code, local MAC address, data payload, and check code.

**Algorithm 1** Control algorithm for 2ASK

$i \leftarrow 1$ // $Z_i$ is the current antenna impedance
**while** Symbol is sending **do**
  Wait for $\frac{1}{2\Delta f}$ // $\Delta f$ is the frequency shift
  **if** $D == 1$ **then**
    $i \leftarrow \mathrm{mod}(i+4, 8)$ // $D$ is the symbol to be sent
  **end if**
**end while**

**Algorithm 2** Control algorithm for 2FSK

$i \leftarrow 1$ // $Z_i$ is the current antenna impedance
**while** Symbol is sending **do**
  **if** $D == 0$ **then**
    Wait for $\frac{1}{8f_1}$ // $f_1 + f_c$ represents symbol 0
  **end if**
  **if** $D == 1$ **then**
    Wait for $\frac{1}{8f_2}$ // $f_2 + f_c$ represents symbol 1
  **end if**
  $i \leftarrow \mathrm{mod}(i+1, 8)$
**end while**

**Algorithm 3** Control algorithm for 2PSK

**if** $D == 0$ **then**
  $i \leftarrow 1$
  // The phase of $Z_1$'s reflection coefficient represents
  // symbol 0
**end if**
**if** $D == 1$ **then**
  $i \leftarrow 5$
  // The phase of $Z_5$'s reflection coefficient represents
  // symbol 1
**end if**
**while** Symbol is sending **do**
  Wait for $\frac{1}{8\Delta f}$ // $\Delta f$ is the frequency shift
  $i \leftarrow \mathrm{mod}(i+1, 8)$
**end while**

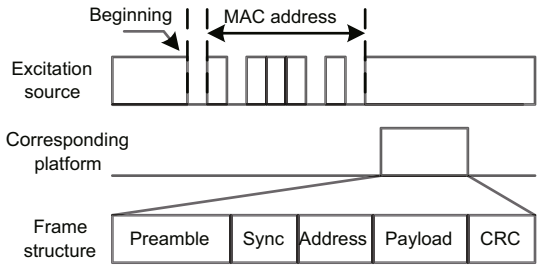


**Fig. 3 Time sequence of the network and frame structure (Sync: synchronous code; CRC: cyclic redundancy check)**

### 3.5 Evaluation

#### 3.5.1 Implementation

Our backscatter-based SDR prototype consists of an energy-harvesting module with an envelope detector, an RF switch, and a baseband controller. Specifically, the energy-harvesting circuit uses the P2110 module, and we can achieve envelope detection by monitoring the voltage of the module's rectifier output. We used the low-power RF switch (i.e., model ADG902) and the low-power FPGA (i.e., model IGLOO AGLN250) to realize the modulation. We implemented ASK, PSK, and FSK modulation algorithms on the FPGA to verify the performance under the corresponding modulation algorithms, and also implemented Hamming codes to verify the performance under error correction coding.

We also implemented an RF power source and a wireless receiver using the SX1276 transceiver with the STM32L152 board. To enable sufficient RF power supply, we used a power amplifier, model ZHL42+, to amplify the signal to 29 dBm.

#### 3.5.2 Experimental setup

We tested the energy harvesting performance with a signal transceiver based on the SX1276 transceiver and a directional antenna. The experimental setup is shown in Fig. 4. The backscatter-based SDR was totally battery-free and was powered by a wireless signal from the transceiver. We used an oscilloscope, model RIGOL MSO5152-E, to measure the charging and discharging time, which indicates the power consumption of our system.

#### 3.5.3 Evaluation results

The results are shown in Fig. 5. We used a 100-mF super-capacitor for energy storage. In sleep mode, the energy stored in the super-capacitor can support our nodes for 613 s. In active mode, the energy stored in the super-capacitor can support our nodes for 2.38 s. We also evaluated the charging period, where the capacitor can be fully charged in 60 s at a distance of 1 m. In practice, the system can work for a longer period of time by entering active mode for just a few tens of milliseconds at a time to complete the data transfer, and then enter sleep mode to save energy.

To evaluate the performance of our design

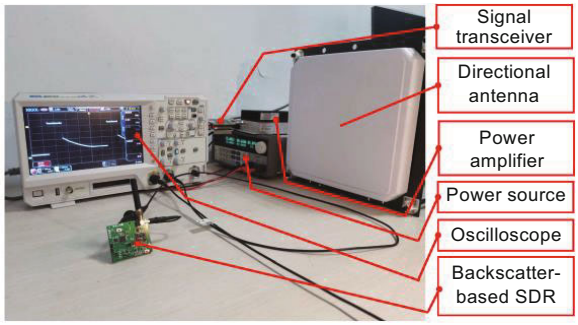


**Fig. 4 Experimental setup**

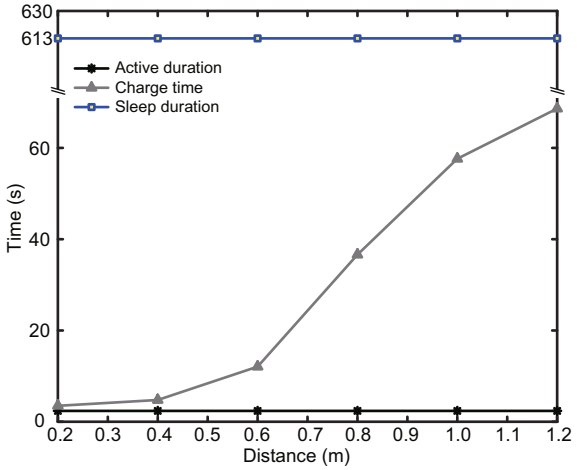


**Fig. 5 Energy harvesting performance**

against the traditional method which uses active components like an oscillator and a multiplier, we presented the BER results by comparing the conventional modulation and backscatter-based modulation in Fig. 6. In ASK modulation, the traditional modulation and backscatter-based modulation have a similar effect. However, in FSK and PSK modulations, we accepted that the conventional modulation is better than the backscatter-based modulation with a low SNR. Still, when the SNR is high, their performances can be comparable. Furthermore, we can use error-correcting code, interleaving, and repetition to obtain more reliable data. We used Hamming(7, 4) code and evaluated its performance as shown in Fig. 6. The results show that for the same BER, the communication method with Hamming coding can achieve a higher SNR. This is especially significant in the case of low SNRs, which also means that a longer communication distance can be obtained with the Hamming coding method.

According to our evaluation results, we can achieve 500 kb/s data transmission in a maximum of 2 s and can transmit data within 1 ms after waking

up. In low-power and low-cost IoT application scenarios, the microsecond-level time to achieve wake-up and hundreds of kb/s level communication rate already meet the application requirements; transmission delay that is accurate to the microsecond level is not significant for the communication scenario.

## 4 Case studies on potential applications of backscatter communication

Passive backscatter technology is an emerging technology with a communication method similar to traditional RFID communication technology. By adapting to multiple protocols, backscatter systems can achieve a more extended communication distance and a higher communication rate than standard RFID. In this section, we discuss backscatter node application scenarios to show the significance of the SDR platform designed in this study at the application level.

### 4.1 Case study on railway monitoring

China's high-speed railways exceeded 140 000 km by the end of 2020 (People's Daily, 2021). With the need to improve railway operation efficiency and competitiveness, railway line information monitoring and maintenance methods urgently need development. Because the backscatter technology holds the characteristics that the batteries are not required, communication protocols can be customized and communications can extend over longer distances than the conventional RFID technology. Therefore, it is suitable to apply backscatter technology in this scenario.

We also developed sensor-loadable passive backscatter nodes for use as sensor monitoring nodes along the railroad, based on the proposed communication platform. We also developed a drone monitoring system that is based on Raspberry Pi and a commercial wireless IoT gateway, which is mounted on a DJI M600 drone. The system is shown in Fig. 7.

Based on the adjustment and modification of the LoRa protocol and ASK modulation method, we designed a set of communication protocols suitable for this scenario. We achieved reading and writing of the ground backscatter node when the UAV was 50 m above the ground with a data rate up to 1 kb/s.

The passive communication performance indicators of the backscatter nodes met the China Railway Siyuan Survey and Design Group acceptance criteria. The acceptance test was completed in the actual

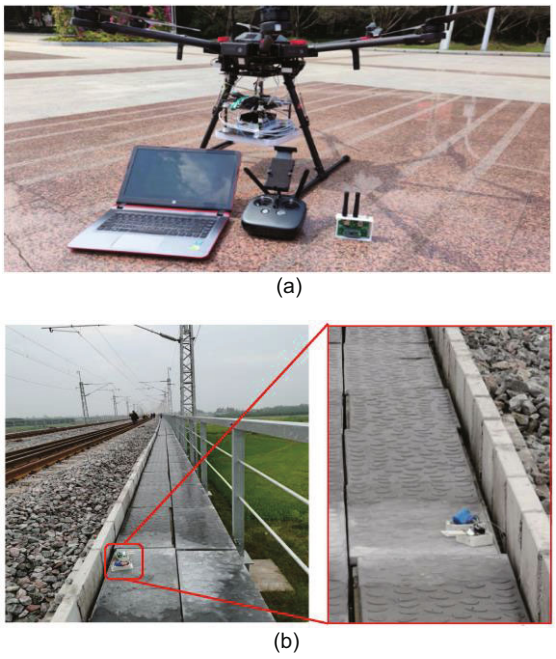


**Fig. 7 Case study on railway monitoring: (a) railway sensor monitoring system; (b) deployment test on railway**

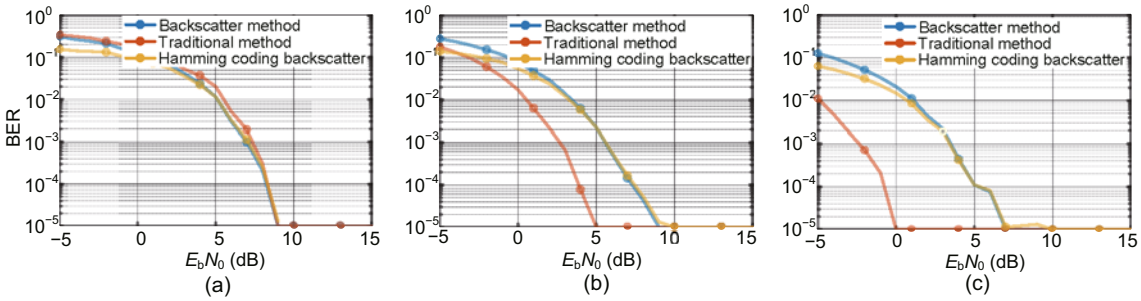


**Fig. 6 Comparison of modulation results between the traditional method and backscatter-based method: (a) ASK; (b) FSK; (c) PSK**

railway section in Xiantao, China. A UAV hung on the 30-dBm excitation source with a 20-dB directional antenna to charge the node. Then we obtained the charging time, communication distance, communication rate, and other parameters. The measured charging period was 120 s, the communication rate was 100 kb/s, and the communication distance was 50 m.

### 4.2 Case study on logistics distribution

Today, major e-commerce corporations need to operate the most sophisticated logistics networks that have never existed.

According to the statistics (Zhao RJ et al., 2020), e-commerce companies such as Alibaba, JD.com, and Amazon need to handle more than 87 billion packages each year, and most of them are currently marked and managed by RFID. However, RFID has exposed problems involving short communication distance, easy loss, and misreading during use. In contrast, backscatter communication technology allows customization of the communication protocol and achieves a longer communication distance and a higher communication rate. Furthermore, the concurrent decoding scheme (Huang et al., 2020) and physical layer synchronization method (Dunna et al., 2021) are expected to replace traditional RFID tags in logistics distribution systems. In recent years, there has been research on backscatter node positioning algorithms as well (Zhang XN et al., 2020). Introducing positioning algorithms can open up a more comprehensive range of applications for backscatter nodes.

Based on our SDR platform, we can simulate and analyze the potential use of backscatter nodes in logistics distribution applications, for example, warehouse management. As shown in Fig. 8, in a warehouse used as temporary transit storage, different packages are stacked together. Wireless identification and location are needed to meet inventory management requirements. In addition, some packages may be sensitive to temperature, and others may be sensitive to humidity. Therefore, it is necessary to design a backscatter SDR platform that is compatible with multiple protocols and multiple sensing methods. Backscatter-based SDR provides interfaces for different IoT sensors, and it is compatible with many wireless protocols, providing much better coverage than NFC and RFID. As shown in Table 3, backscatter communication provides larger area coverage and is more compatible with wireless communication protocols. Our team has set some related directions and will continue to work on associated industries for further research.

### 4.3 Case study on intelligent factories

Industry 4.0 aims to transform traditional manufacturing and industrial practices with 5G, advanced automation, artificial intelligence, and IoT technologies. Intelligent factories have many new requirements, such as the control and positioning of robotic arms and the monitoring and position perception of goods. Unlike the EPC Gen2 protocol, which is widely used in linear commercial RFID, backscatter technology, combined with various existing IoT communication protocols, can complete tasks such as communication and perception. For example, Aloba (Guo et al., 2020) uses a backscatter node to reflect the LoRa signal to monitor the vibration of mechanical equipment in the factory. LTE

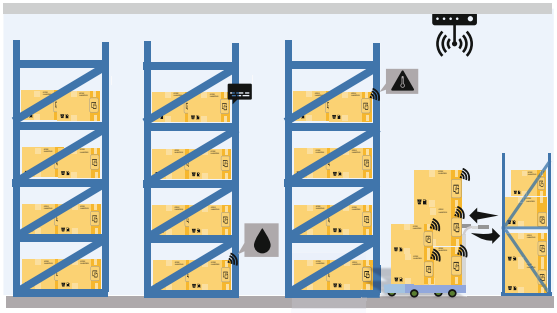

**Fig. 8 Potential use of backscatter-based SDR nodes in logistics distribution systems**

**Table 3 Comparison of technologies used for identification and localization in logistics distribution systems and intelligent factories**

| Technology | Communication distance | Localization | Protocol support |
|---|---|---|---|
| RFID | <10 m | Yes | Gen2 |
| NFC | <0.1 m | No | NFCIP-I |
| Backscatter | Up to 1.8 km | Yes | LoRa, ZigBee, 802.11, etc. |

backscatter (Chi et al., 2020) can monitor goods, descriptions, and vehicle information.

Based on our SDR platform, we can easily simulate and analyze applications in an intelligent factory. As shown in Fig. 9, our platform can be attached to cargo on the assembly line for accurate identification and localization. Our technology also allows longer communication distances for robots and battery-free backscatter tags than RFID technologies, and thus facilitates positioning and identification in a larger space. Also, existing positioning methods (Nandakumar et al., 2018; Luo et al., 2019) based on backscatter technology can be applied to our platform, which also has greater potential in industrial process control.

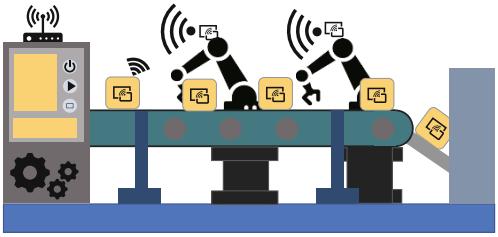

**Fig. 9 Potential use of backscatter-based SDR nodes in intelligent factories**

## 5 Discussion

We sum up the limitations and opportunities of the backscatter-based SDR, as discussed below:

1. Amplitude modulation. Instead of using a multiplier for signal synthesis, the backscatter-based SDR generates signals through on-off switching. Because of this limitation, it cannot achieve multi-stage modulation on amplitude. Thus, modulation methods such as quadrature amplitude modulation (QAM) cannot be used on our platform with an ambient single carrier. However, we can achieve QAM modulation to some extent, if we use the QAM-modulated signal as a carrier. For example, Moxcatter (Zhao J et al., 2018) takes a more in-depth look at using backscatter to reflect 802.11n signals, which are QAM modulated.

2. Communication distance. The scattering process introduces a lot of attenuation in re-radiated signals. The propagation distance of the reflected signal is smaller than that of conventional active nodes, but backscatter still holds great promise in terms of energy efficiency. In the same battery-free condition, backscatter-based SDR achieves a longer communication range than RFIDs, which provides a considerable number of application scenarios.

3. Downlink sensitivity. The backscatter-based SDR uses envelope detection in downlinks. Due to the poor sensitivity of the envelope detector (Talla et al., 2021), the communication distance and communication rate in the downlink are greatly limited.

## 6 Concluding remarks and future directions

This study takes the first step toward SDR design by employing μW-level backscatter technology for battery-free IoT nodes. We hope that the design can contribute to ultra-low-power SDR design for large-scale simplified and intelligent IoT networks, and promote relevant research in the following directions:

1. Energy efficiency management during communication. We present opportunities for researchers to evaluate the power efficiency of their wireless communication algorithm.

2. Large-scale passive backscatter network management. We promote a battery-free platform for IoT networks that enables further studies and exploration of the IoT network structure and corresponding communication protocols.

3. Concurrent communication and sensing in passive backscatter networks. Concurrent passive communication in factories and logistics is a research hotspot. It is hard to simulate real communication scenarios with traditional power-stable SDRs. Our platform provides opportunities for research into communication schemes in unstable power conditions.

### Contributors

Huixin DONG, Wei KUANG, Fei XIAO, and Wei WANG designed the research. Wei KUANG processed the data. Huixin DONG and Wei KUANG drafted the paper. Fei XIAO, Lihai LIU, Feng XIANG, Wei WANG, and Jianhua HE helped organize the paper. Huixin DONG and Wei KUANG revised and finalized the paper.

### Compliance with ethics guidelines

Huixin DONG, Wei KUANG, Fei XIAO, Lihai LIU, Feng XIANG, Wei WANG, and Jianhua HE declare that they have no conflict of interest.

## References


Analog Devices, 2016. ADG904 Datasheet. https://www.analog.com

Avx, 2020. Avx BestCap. http://catalogs.avx.com/BestCap.pdf

Chi ZC, Liu X, Wang W, et al., 2020. Leveraging ambient LTE traffic for ubiquitous passive communication. Proc Annual Conf of the ACM Special Interest Group on Data Communication on the Applications, Technologies, Architectures, and Protocols for Computer Communication, p.172-185. https://doi.org/10.1145/3387514.3405861

Dunna M, Meng M, Wang PH, et al., 2021. SyncScatter: enabling WiFi like synchronization and range for WiFi backscatter communication. Proc 18th USENIX Symp on Networked Systems Design and Implementation, p.923-937.

Ettus, 2018. USRP B200mini-i. https://www.ettus.com/all-products/usrp-b200mini-i-2/

Guo XZ, Shangguan LF, He Y, et al., 2020. Aloba: rethinking ON-OFF keying modulation for ambient LoRa backscatter. Proc 18th Conf on Embedded Networked Sensor Systems, p.192-204. https://doi.org/10.1145/3384419.3430719

Hessar M, Najafi A, Iyer V, et al., 2020. TinySDR: low-power SDR platform for over-the-air programmable IoT testbeds. 17th USENIX Symp on Networked Systems Design and Implementation, p.1031-1046.

Huang QY, Song GC, Wang W, et al., 2020. FreeScatter: enabling concurrent backscatter communication using antenna arrays. *IEEE Int Things J*, 7(8):7310-7318. https://doi.org/10.1109/JIOT.2020.2984877

Kuo YS, Pannuto P, Schmid T, et al., 2012. Reconfiguring the software radio to improve power, price, and portability. Proc 10th ACM Conf on Embedded Network Sensor Systems, p.267-280. https://doi.org/10.1145/2426656.2426683

LimeNet, 2018. LimeSDR. https://limemicro.com/products/boards/limesdr/

Luo ZH, Zhang QP, Ma YF, et al., 2019. 3D backscatter localization for fine-grained robotics. Proc 16th USENIX Conf on Networked Systems Design and Implementation, p.765-781.

Microsemi, 2012. AGLN250 Datasheet. https://cn.alldatasheet.com/view.jsp?Searchword=AGLN250

muRata, 2018. muRata Lumped Compent. https://www.murata.com/zhcn/support/faqs/capacitor/ceramiccapacitor/char/0039

Nandakumar R, Iyer V, Gollakota S, 2018. 3D localization for sub-centimeter sized devices. Proc 16th ACM Conf on Embedded Networked Sensor Systems, p.108-119. https://doi.org/10.1145/3274783.3274851

Peng Y, Shangguan LF, Hu Y, et al., 2018. PLoRa: a passive long-range data network from ambient LoRa transmissions. Proc Conf of the ACM Special Interest Group on Data Communication, p.147-160. https://doi.org/10.1145/3230543.3230567

People's Daily, 2021. Chinese Railway Operating Mileage. http://www.gov.cn/xinwen/2021-09/26/content5639361.htm [Accessed on Sept. 26, 2021].

Philipose M, Smith JR, Jiang B, et al., 2005. Battery-free wireless identification and sensing. *IEEE Perv Comput*, 4(1):37-45. https://doi.org/10.1109/MPRV.2005.7

SiTime, 2017. SiT1576 Datasheet. https://www.sitimechina.com

Talla V, Hessar M, Kellogg B, et al., 2017. LoRa backscatter: enabling the vision of ubiquitous connectivity. Proc ACM on Interactive, Mobile, Wearable and Ubiquitous Technologies, p.1-24. https://doi.org/10.1145/3130970

Talla V, Smith J, Gollakota S, 2021. Advances and open problems in backscatter networking. *GetMob Mob Comput Commun*, 24(4):32-38. https://doi.org/10.1145/3457356.3457367

TI, 2018a. TPL5111 Datasheet. https://www.ti.com

TI, 2018b. TPS782xx LDO. https://www.mouser.com/Texas-Instruments/LDO-Voltage-Regulators/TPS78218-Series/N-1z0zls6Z5cgacZ1yxywu6

Zhang P, Peng MG, Cui SG, et al., 2022. Theory and techniques for "intellicise" wireless networks. *Front Inform Technol Electron Eng*, 23(1):1-4. https://doi.org/10.1631/FITEE.2210000

Zhang PY, Bharadia D, Joshi K, et al., 2016. HitchHike: practical backscatter using commodity WiFi. Proc 14th ACM Conf on Embedded Network Sensor Systems CD-ROM, p.259-271. https://doi.org/10.1145/2994551.2994565

Zhang XN, Wang W, Xiao XD, et al., 2020. Peer-to-peer localization for single-antenna devices. Proc ACM on Interactive, Mobile, Wearable and Ubiquitous Technologies, p.1-25. https://doi.org/10.1145/3411833

Zhao J, Gong W, Liu JC, 2018. Spatial stream backscatter using commodity WiFi. Proc 16th Annual Int Conf on Mobile Systems, Applications, and Services, p.191-203. https://doi.org/10.1145/3210240.3210329

Zhao RJ, Wang PR, Ma YF, et al., 2020. NFC+: breaking NFC networking limits through resonance engineering. Proc Annual Conf of the ACM Special Interest Group on Data Communication on the Applications, Technologies, Architectures, and Protocols for Computer Communication, p.694-707. https://doi.org/10.1145/3387514.3406219